Available online www.jocpr.com

Journal of Chemical and Pharmaceutical Research, 2013, 5(12):1083-1088

Research Article

ISSN : 0975-7384
CODEN(USA) : JCPRC5

The research on petrochemistry components mapping with ASTER data

Ming Tao*[1,2], Zhang Wenshan[3] and Peng Guangxiong[3]

[1]College of Civil Engineering & Architecture, China Three Gorges University, Daxue Street, Xiling District, Yichang City, Hubei Province, China
[2]National Field Observation and Research Station of Landslides in Three Gorges of Yangtze River, China Three Gorges University, Daxue Street, Xiling District, Yichang City, Hubei Province, China
[3]Central South University, Lu Shan Nan Street, Yuelu District, Changsha City, Hunan Province, China

---

ABSTRACT

ASTER Data have high spectral resolution and can be used to quickly mapping on a variety of mineral alteration .The pertrochemistry components in an area in Ethiopia were chosen as experimental targets. Eight types of mineral alteration were extracted using method of PCA and band ratio from ASTER data. Each type of mineral alteration was divided into three levels. Finally the petrochemistry components maps were finished. They provid guidance for further geological prospecting work .

Key words: Alteration extraction, Petrochemistry components, ASTER

INTRODUCTION

Anomaly alteration information can be extracted from TM data successfully by using the principal component analysis(PCA) technique and Crosta rule[1].But the spectral resolution of TM is limited. Their three types of bands in TM including visible and near-infrared (VNIR) and shortwave infrared (SWIR) bands. This means that only iron-oxide and hydroxyl anomaly alteration information can be extracted. The higher spectral resolution remote sensing data are needed in petrochemistry components mapping.

Table1. Bands characteristics of ASTER sensor

Group	Band	Spectral range(μm)	Resolution
VNIR	1	0.52-0.60	15
	2	0.63-0.69	
	3N	0.78-0.86	
	3B	0.78-0.86	
SWIR	4	1.60-1.70	30
	5	2.145-2.185	
	6	2.185-2.225	
	7	2.235-2.285	
	8	2.295-2.365	
	9	2.36-2.43	
TIR	10	8.125-8.475	90
	11	8.475-8.825	
	12	8.925-9.275	
	13	10.25-10.95	
	14	10.95-11.65	

ASTER is the Advanced Spaceborne Thermal Emissilican and Reflection Radiometer, a multi-spectral sensor onboard one of NASA's Earth Observing System satellites, Terra, which was launched in 1999[2]. There are three groups of bands in ASTER sensor including VNIR,SWIR and thermal infrared radiation (TIR). The bands characteristics are presented in Table1.

According to early studies, A. P. Crosta extracted alunite, illite, kaolinite+smectite and kaolinite using ASTER imagery and principal component analysis[3]. Lv Fengjun and his collaborators rebulit alteration mineralization spectral curves on ASTER remote sensing data based on representative alteration minerals reflectivity data in USGS standard spectral database. They extracted Al-OH, Mg-OH and CO_3^{2-} from ASTER data[4]. Aleks Kalinowski and Simon Oliver provided Commonly used ASTER band ratios and band combinations[5].

Since the 1990 s, ASTER data have been used in a variety of types of mineral exploration including epithermal gold deposits, laterite nickel deposits, copper polymetallic deposits etc[6-9].

We chose an area as the experimental area in Ethiopia. Ethiopia is a country located in the northeast of Africa with rich metallic mineral resources. The terrain in experimental area is varied and ups and downs with sparse vegetation. It is very suitable for remote sensing data acquisition, processing and interpretation. There is good metallogenic geological conditions in experimental and many outcrops were discovered in the previous geological work. So it is an ideal experimental area.

EXPERIMENTAL SECTION

The area of experimental area is about 1400 square kilometers. Iron-oxide, Al-OH, Mg-OH, alunite, illite, kaolinite, sericite and silica were chosen as the research targets. Alteration information of Iron-oxide, Al-OH, Mg-OH, alunite, illite, kaolinite, sericite were extracted by PCA and silica was band ratio[3-5]. ASTER data processing and mapping used software of ENVI4.5.

The experiment was divided into four steps. The first step was to get the experimental ASTER data covering experimental area. The second step was data pre-processing. Next step was alteration extraction. The extraction methods are PCA and band ratio. The forth step was anomaly alteration information classification. Anomaly alteration information were divided into three levels by thresolding technique[10].The last step was petrochemistry components mapping. The flow diagram is presented in Figure 1.

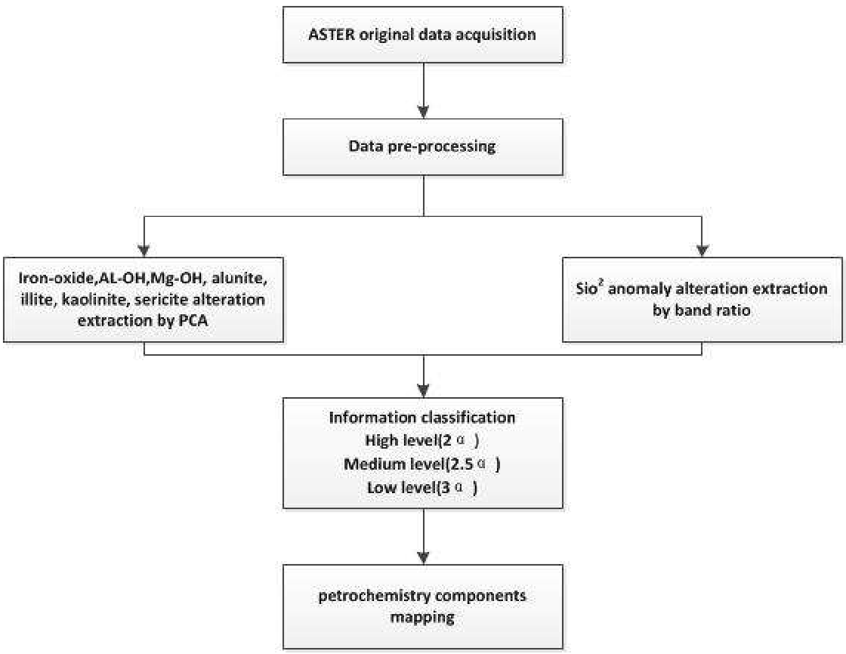

Figure 1: Flow Diagram of Experiment

ASTER data acquisition and data pre-processing

ASTER data bought from data provider. We got two scenes of ASTER data with ID of ASTL1A0703100808570703140253 and ASTL1A0602190807330602210564.Data pre-processing includes data cropping, geometric correction and atmospheric correction. The precisilican of geometric correction was under 1 pixel.

Anomaly alteration extraction by PCA
Iron-oxide, Al-OH, Mg-OH, alunite, illite, kaolinite, sericite alteration were extracted by PCA. The alteration types and the ASTER bands used to extract information are presented in Table 2.

Table 2. Alteration and types and ASTER bands

Alteration types	ASTER bands
iron-oxide	1,2,3,4
Al-OH	1,3,4,5
Mg-OH	1,3,4,8
alunite	1,4,6,7
illite	1,3,5,6
kaolinite	1,3,5,7
sericite	1,4,6,9

The PCA eigenvector loadings of each alteration type are presented in Table 3 to Table 9.

Table 3. Iron-oxide alteration extraction PCA eigenvector loadings table

	Band1	Band2	Band3	Band4
PC1	0.411070	0.234331	0.682904	0.556554
PC2	0.909540	-0.051631	-0.342181	-0.230183
PC3	0.017295	-0.747423	-0.254029	0.613620
PC4	0.058820	-0.619502	0.593316	-0.510621

Table 4. Al-OH alteration extraction PCA eigenvector loadings table

	Band1	Band3	Band4	Band5
PC1	0.249355	0.506134	0.650358	0.508611
PC2	0.404259	0.714915	-0.375443	-0.429551
PC3	0.709877	-0.321250	-0.399731	0.482792
PC4	-0.520069	0.359893	-0.525635	0.568958

Table 5. Mg-OH alteration extraction PCA eigenvector loadings table

	Band1	Band3	Band4	Band8
PC1	0.246155	0.494725	0.632544	0.542718
PC2	0.393880	0.733879	-0.392559	-0.390099
PC3	0.555804	-0.261528	-0.520568	0.593038
PC4	0.689455	-0.385060	0.418084	-0.448983

Table 6. Alunite alteration extraction PCA eigenvector loadings table

	Band1	Band3	Band5	Band7
PC1	0.274481	0.536185	0.546467	0.581842
PC2	0.350150	0.717080	-0.431337	-0.420880
PC3	-0.883512	0.442536	0.116286	-0.100235
PC4	0.146501	-0.049642	0.708379	-0.688675

Table 7. Illite alteration extraction PCA eigenvector loadings table

	Band1	Band3	Band5	Band6
PC1	0.265353	0.525221	0.539622	0.602112
PC2	0.355049	0.726400	-0.399440	-0.432124
PC3	0.896176	-0.443265	-0.017996	0.007840
PC4	-0.019920	0.001680	-0.740900	0.671318

Table 8. Kaolinite alteration extraction PCA eigenvector loadings table

	Band1	Band4	Band6	Band7
PC1	0.220066	0.614141	0.547891	0.523658
PC2	0.961337	-0.242432	-0.129628	0.015950
PC3	-0.134234	-0.750468	0.463591	0.451510
PC4	-0.096868	0.029229	-0.684175	0.722265

Table 9. Sericite alteration extraction PCA eigenvector loadings table

	Band1	Band4	Band6	Band9
PC1	0.231634	0.645294	0.574129	0.447568
PC2	0.951574	-0.266625	-0.137156	0.067877
PC3	-0.165741	-0.707087	0.471986	0.499787
PC4	-0.115686	0.111963	-0.654823	0.738436

Silica alteration were extracted by band ratio. The bands statistical table presented in Table 10.

Table 10.Silica alteration extraction bands statistical table

	Min	Max	Mean	Stdev
ASTER12	0	11.70088	7.521708	4.43045
ASTER14	0	10.99442	7.286081	4.28691

Information classification and petrochemistry components mapping

Anomaly alteration information was divided into three levels by the multiple of standard deviation of principal component image. Anomaly alteration principal component image standard deviation α was selected as classification index. Three levels are 2α, 2.5α and 3α. Different colors re[resent different levels in petrochemistry components map. Red represented high level. Green represented medium level. Blue represented low level.

RESULTS AND DISCUSSION

Analysis of alteration PCA eigenvector loadings

In Iron-oxide alteration extraction PCA eigenvector loadings table, the sign of band1 and band3 are positive and they are opposite to band2 and band4 in PC4. According to Crosta rule, the Iron-oxide anomaly alteration principal component is PC4 and the bright pixels present the Iron-oxide Iron-oxide alteration.

In Al-OH alteration extraction PCA eigenvector loadings table, the sign of band4 is negative and is opposite to band5 in PC4. The alteration principal component is PC4 and the dark pixels present Al-OH anomaly alteration.

In Mg-OH alteration extraction PCA eigenvector loadings table, the sign of band4 is positive and is opposite to band8 in PC4. The alteration principal component is PC4 and the bright pixels present Mg-OH anomaly alteration.

In alunite alteration extraction PCA eigenvector loadings table, the sign of band5 is positive and is opposite to band7 in PC4. The alteration principal component is PC4 and the bright dark present alunite anomaly alteration.

In illite alteration extraction PCA eigenvector loadings table, the sign of band5 is negative and is opposite to band6 in PC4. The alteration principal component is PC4 and the bright dark present illite anomaly alteration.

In kaolinite alteration extraction PCA eigenvector loadings table, the sign of band6 is negative and is opposite to band7 in PC4. The alteration principal component is PC4 and the bright present kaolinite anomaly alteration.

In sericite alteration extraction PCA eigenvector loadings table, the sign of band6 is negative and is opposite to band9 in PC4. The alteration principal component is PC4 and the bright present sericite anomaly alteration.

Petrochemistry components mapping results

According to the above analysis, the standard deviation of each principal component image was calculated. Each alteration map was completed according to classification index. The result maps are present in Figure2 to Figure 9.

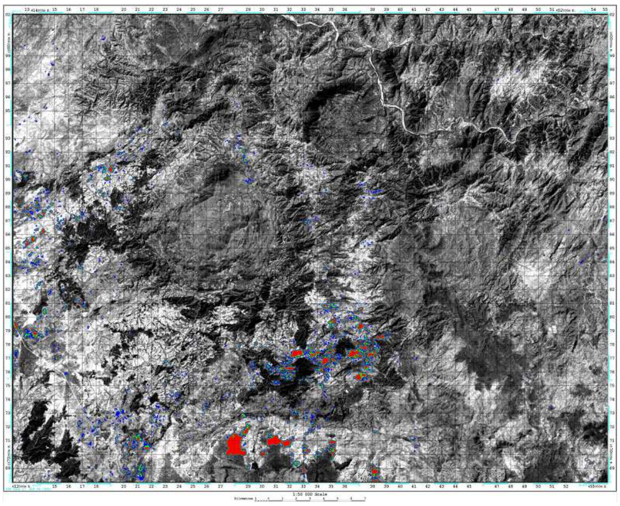

Figure 2: Iron-oxide alteration distribution map

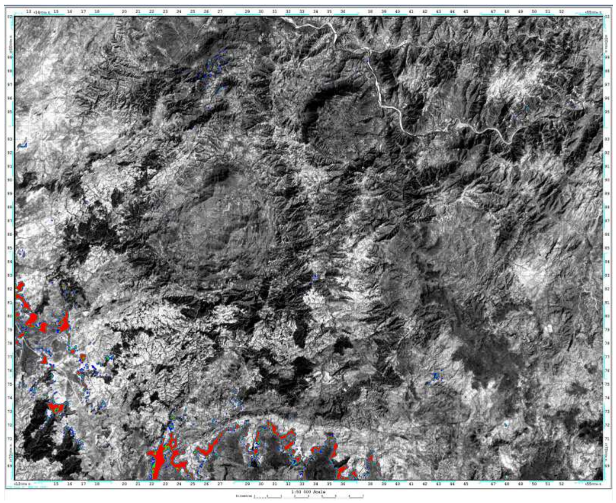

Figure 3: Al-OH alteration distribution map

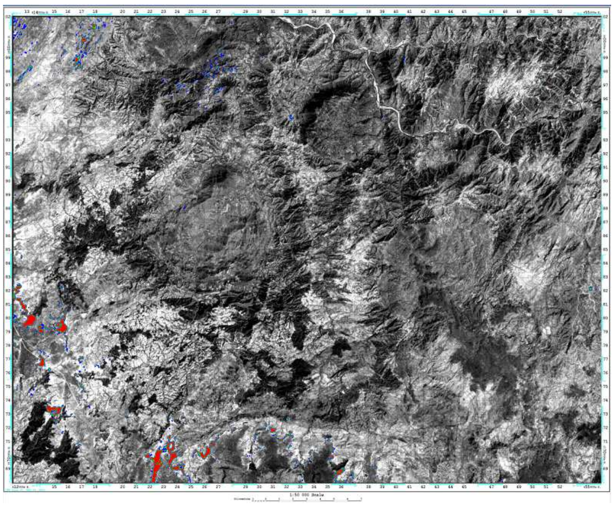

Figure 4: Mg-OH alteration distribution map

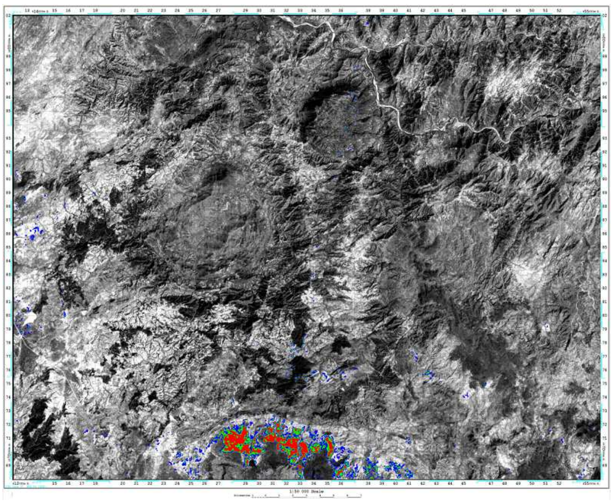

Figure 5: Al-OH alunite distribution map

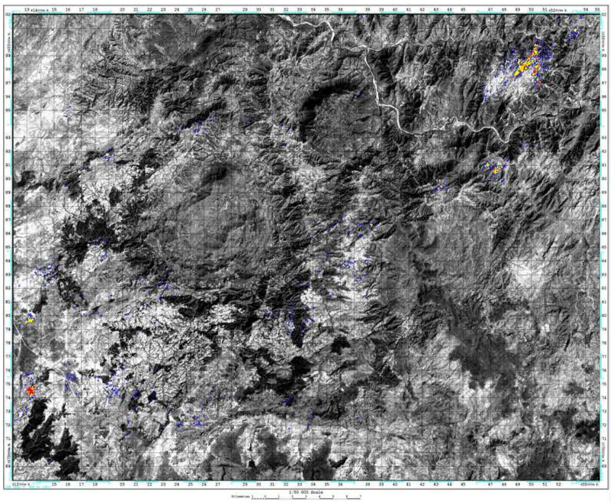

Figure 6: Illite alteration distribution map

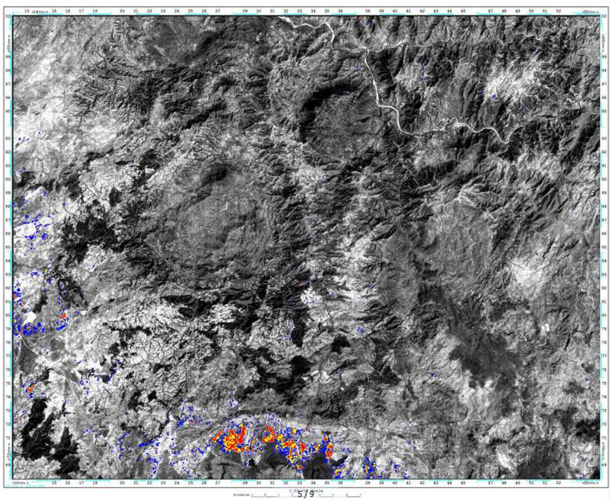

Figure 7: Kaolinite alunite distribution map

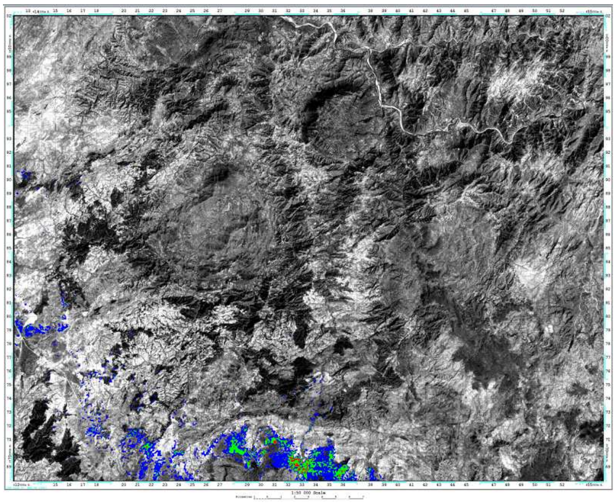

Figure 8: Sericite alteration distribution map

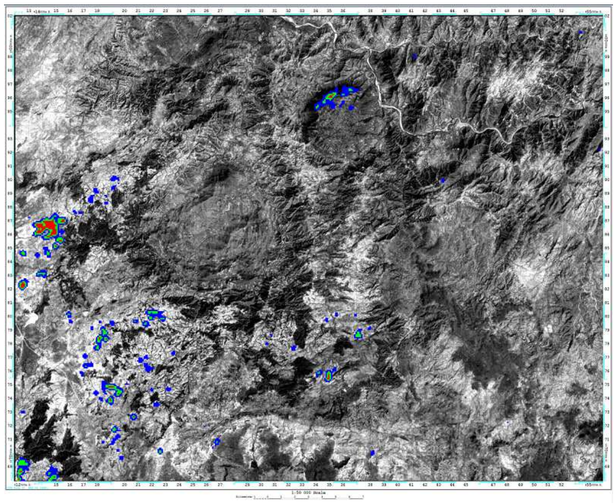

Figure 9: Silica alunite distribution map

CONCLUSION

ASTER data have higher spectral resolution then TM data and can identify more minerals. Eight types of alteration including iron-oxide, Al-OH, Mg-OH, alunite, illite, kaolinite, sericite and silica alteration were easily extracted because of abundant spectral information in ASTER data. PCA and band ratio are convenient and feasible methods to extracted alteration. ASTER data and these extraction methods provide us simple and fast petrochemistry components mapping technique. It is very meaningful for geological prospecting work in large area.

In addition, considering bands and band ratios do not indicate the occurrence of a mineral with absolute certainty or with any idea of quantity, the ground work is still indispensable.

REFERENCES

[1] W P Loughlint. *Photogrammetric Engineering & Remote Sensing.* **1991**,57, 1163–1169. CROSTA A P;MOORE J MCM.*Proceedings of the 9th Thematic Conference on Remote Sensing for Exploration Geology, Calgary (Ann Arbor, MI: Environmental Research Institute of Michigan)*,**1985**,1173–1187.
[2] Yan Shouxun;Zhang Bing;Zhao Yongchao;*Remote Sensing Techniques and Application*, **2004**, 19 (1): 52-63.
[3] Crosta A P;DucartD F; Carlos Roberto;De Souza Filho.*Reviews in Economic Geology*, **2009**, 16: 97-108.
[4] Crosta A P;Souza Filho C R;Azevedo F.*International Journal of Remote Sensing*, **2003**, 24: 4233-4240.
[5] Seoane JC S;Castro N A;Osako L S.*Reviews in Economic Geology*, **2009**, 16,109-122.
[6] Ma Jianwen.*Journal of Remote Sensing*,**1997**,3,22-26.
[7] Zhang Yujun;Yang Jianmin;Chen Bi.*National Resource Remote Sensing*, **2002**,4,30-36.
[8] Dai Jingjing;Qu Xiaoming;Xin Hongbo. *Geological bulletin of China*.**2010**,29(5),752-759.
[9] Zhang Yujun;Yang Jianmin;Chen Wei. *Remote Sensing for land & resouces.***2003**,2(56),44-49.